

## Properties of Fractal Colloid Aggregates

**H. M. Lindsay, M. Y. Lin,<sup>†</sup> D. A. Weitz,\* P. Sheng and Z. Chen<sup>†</sup>**  
*Exxon Research and Engineering, Rt 22 E, Annandale, NJ 08801, U.S.A.*

**R. Klein**

*Department of Physics, University of Konstanz, Konstanz, Federal Republic of Germany*

**P. Meakin<sup>‡</sup>**

*Department of Physics, Boston University, Boston, MA 02140, U.S.A.*

We study the influence of the fractal structure on the physical properties of colloidal gold aggregates. The optical properties are strongly influenced by both the long- and the short-range correlations of the aggregate structure, as well as the electronic plasma resonance of the gold particles. The absorption of the aggregates is dominated by the electromagnetic interaction between nearest-neighbour particles. The angular dependence of the polarized scattering reflects the long-range fractal correlations of the particles in the clusters, while that of the depolarized scattering reflects the short-range correlations of the local field corrections. The fractal structure also affects dynamic light scattering, so that rotational diffusion effects play an important role in the decay of the autocorrelation function. Finally, we show that the very tenuous nature of the fractal structure makes the aggregates quite susceptible to deformation under shear stress.

There have been considerable advances recently in our understanding of the process of colloid aggregation.<sup>1</sup> Central to all this work is the recognition that the highly disordered structure of colloidal aggregates can be characterized in quantitative terms. It has been shown both experimentally<sup>2</sup> and through computer simulation<sup>3,4</sup> that the structure of colloidal aggregates exhibits scale invariance and can be quantitatively described as a fractal. This development has been accompanied by significant advances in our understanding of the dynamics of the aggregation process and the causal relationship with the structure.<sup>5,6</sup> Thus a new and rather elegant picture of colloid aggregation is emerging.

Armed with the new knowledge of the process of colloid aggregation, an important set of questions can now be investigated. Since we can quantitatively characterize the structure of colloidal aggregates, we can investigate their physical properties in much greater detail. Of particular interest is the determination of the physical properties unique to fractal objects. Knowledge of these is crucial not only as a matter of fundamental scientific interest, but also because of the technological importance of colloidal flocs.

In this paper we examine several different aspects of the physical properties of colloidal aggregates that are uniquely affected by the fact that their structure is fractal. These properties include a detailed discussion of the optical properties as well as the results of a preliminary investigation of the mechanical stability of the fractal structure. We study the properties of colloidal gold aggregates. Colloidal gold has historically been a widely studied system and is a prototypic lyophobic, metal colloid. It has the advantage that the aggregation process has been studied in considerable detail and is

<sup>†</sup> Also at the Department of Physics, City College of CUNY, New York, NY 10031, U.S.A.

<sup>‡</sup> Permanent address: E. I. DuPont Co., Wilmington, DE, U.S.A.

relatively well understood.<sup>1</sup> Furthermore, the aggregation of gold colloids can be easily controlled, and the fractal dimension of the resultant clusters can be reproducibly varied by changing the conditions of the aggregation kinetics.<sup>5</sup> This gives us additional flexibility in determining the effects of the fractal structure on the physical properties of the aggregates. Colloidal gold also possesses an additional very interesting property, in common with several other, widely studied metal colloid systems. This is the electronic plasma resonance that gives the colloid its unique colours: red when unaggregated and blue or grey when aggregated.<sup>7</sup> In this paper, we also consider the effect of this resonance, in combination with the fractal structure, on the optical properties of the aggregates.

The recent advances in our understanding of the kinetic aggregation process of colloidal gold have been discussed elsewhere,<sup>1</sup> and we present here only a very brief summary. The aggregation of colloidal gold can be divided into two distinct regimes.<sup>5</sup> In the first, the aggregation is very rapid, and the rate is limited solely by the time taken for cluster collisions to occur *via* Brownian diffusion. This is diffusion-limited cluster aggregation<sup>3,4</sup> (DLCA). In the second regime the rate is limited by the low probability of actually forming a bond upon collision of two clusters. This is reaction-limited cluster aggregation<sup>8-10</sup> (RLCA). These regimes are achieved experimentally by adjusting the charge on the colloid surface, and hence the height of the potential barrier caused by the repulsive Coulomb interaction between approaching colloid particles.<sup>6</sup> When the surface charge is completely removed, so there is no repulsive barrier, DLCA results. By contrast, if the surface charge is reduced so the barrier is still several  $k_B T$ , RLCA results.

The clusters in both regimes are fractal, but their fractal dimensions,  $d_f$ , are different.<sup>5</sup> For DLCA,  $d_f \approx 1.8$ , while for RLCA,  $d_f \approx 2.1$ . In addition, both the cluster mass distributions, and their time dependences, are different for each regime.<sup>11</sup> For diffusion-limited aggregation, the cluster mass distribution exhibits a broad peak, and the average cluster mass grows roughly linearly with time.<sup>12</sup> By contrast, for reaction-limited aggregation, the cluster mass distribution is power-law,  $C_M \propto M^{-\tau}$ , with  $\tau \approx 1.5$ , up to some cutoff mass. This cutoff mass (which characterizes the size of the clusters in the distribution) increases exponentially with time. Thus we can use this knowledge of the aggregation of colloidal gold to obtain clusters of a known structure, as characterized by their fractal dimension, and distribution.

Detailed knowledge of the aggregation process also provides us with another valuable method for studying the physical properties of colloidal aggregates. The physics of the aggregation can be formulated as a set of rules and then simulated on a computer. This allows one to generate clusters that have the same fractal dimension and cluster mass distribution as that produced by experiment. Moreover, from the simulations we know the exact coordinates of each particle in the clusters, and these can be used for numerical calculations to determine a variety of physical properties of the clusters. Here we use the results of an off-lattice diffusion-limited cluster-cluster aggregation model<sup>13</sup> for numerical computations.

In this paper we investigate a variety of physical properties of aggregates. Since optical scattering techniques are one of the simplest and most informative methods for studying colloids and aggregation in general, an understanding of the optical properties is crucial. We therefore investigate the optical properties of fractal gold aggregates in detail. We consider the influence of both the structure of the aggregates and the electronic plasma resonance on both the absorption and scattering from the clusters. We also consider the effects of the fractal structure of the aggregates on dynamic light scattering. The size of the aggregates is typically much larger than the inverse of the scattering vector used. We show that this results in a significant contribution from rotational diffusion to the decay of the measured autocorrelation of the scattered light intensity, and we develop a general formalism to properly account for this. Finally, we consider the mechanical properties of the aggregates. A fractal aggregate possesses unique

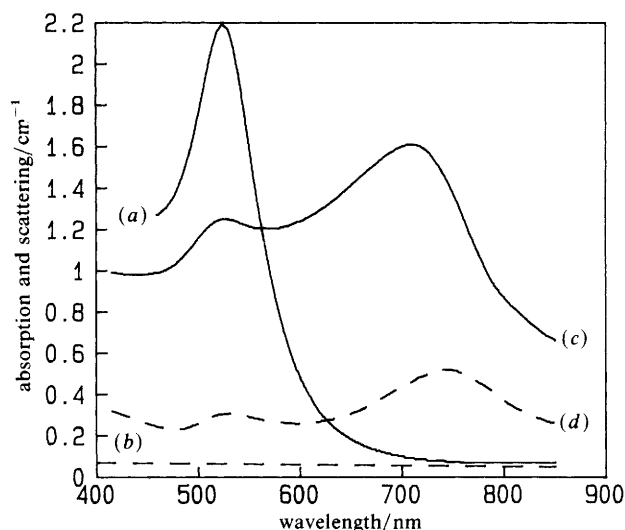


**Fig. 1.** The absorption (solid line) and integrated scattering (dashed line) from unaggregated gold colloids, (a) and (b); and from DLCA colloids, 25 min after the aggregation was initiated, (c) and (d).

correlations, which have significant consequences on its mechanical and structural stability. An understanding of these effects is essential since most colloidal aggregates of technological importance are rarely prepared under the controlled aggregation conditions used in the laboratory. We discuss preliminary measurements of the mechanical stability of colloidal aggregates and the effects of shear forces on their structure.

The remaining paper is divided into four sections. The next section discusses the optical properties of fractal aggregates and the effect of the electronic plasma resonance on these properties. The following section discusses quasielastic scattering from fractal aggregates and the contribution of rotational diffusion to the measured decay time. Then we discuss the changes in the structure of the aggregates induced by shear forces. We present a brief summary in the final section.

## Optical Properties

### Absorption

The optical properties of gold colloidal aggregates are strongly affected by two features: the electronic plasma resonance that is unique to metal colloids and the fractal structure that characterizes clusters formed by irreversible kinetic aggregation. In qualitative terms, the electronic plasma resonance most strongly influences the absorption of the aggregates, while the fractal structure most strongly influences the static scattering properties. However, each of these two phenomena also has some influence on the other property; the plasma resonance on the scattering and the correlations of the fractal structure on the absorption. In this section we discuss these effects.

In fig. 1 we plot both the absorption and the integrated scattering as a function of wavelength for a solution of unaggregated gold colloids and for colloids aggregated by DLCA. These data were obtained using a spectrophotometer fitted with an integrating sphere. Thus the absorption represents the light actually absorbed (transmitted intensity minus scattered intensity), while the scattering represents the total light scattered in all

directions (although there is only appreciable intensity scattered in the forward direction). The measured scattering is corrected for absorption effects. The consequences of the electronic plasma resonance are clearly visible in the absorption of the unaggregated colloids, which has a large peak at *ca.* 530 nm, resulting in the distinct wine-red colour of colloidal gold. The scattered light is so weak that it is almost unmeasurable with this apparatus, reflecting the very small size of the particles and showing how the plasma resonance affects primarily the absorption. As the aggregates grow, an additional absorption resonance develops at longer wavelength, and the scattering intensity increases. The increased absorption at longer wavelengths caused by this new resonance results in the distinctive change in colour of the colloid upon aggregation, from red to blue.

An understanding of the absorption resonances for the aggregated colloid requires an appreciation of the unique correlations between the particles in the cluster.<sup>14</sup> At later times there are few if any monomers remaining, yet there still remains a pronounced and distinct resonance at essentially the same wavelength as for the unaggregated colloid. This implies that both absorption peaks are due to gold particles incorporated within the clusters. While each cluster is comprised of many particles, the long-range structure is fractal, meaning that the average density, or volume fraction of gold in a cluster is quite low. Nevertheless, since the cluster is connected, each particle has on average two near neighbours, resulting in very strong and well defined short-range correlations. It is these latter correlations which predominantly determine the optical resonances.

The shifts and splitting in the electronic plasma resonance evident in fig. 1 arise from the electromagnetic interactions of the resonances on neighbouring particles. An instructive example of this is seen in the calculations for the optical absorption of a dimer.<sup>15</sup> It exhibits two resonances, the excitation of which depend on the orientation of the polarization of the field compared to the axis joining the dimer pair. One resonance is at nearly the same frequency as the single-particle resonance and occurs when the field is polarized normal to the axis joining the two particles. The second is at a lower frequency and occurs when the polarization is parallel to the dimer axis. Physically, the second resonance at longer wavelengths arises from the fact that the electric field extends outside the metal in the narrow gaps which exist when two spheres touch. Thus the near-field coupling between the spheres is basically capacitive in nature and the shift in the resonance has the same physics as that underlying the dielectric anomaly in the Maxwell-Garnet theory.<sup>16</sup> It is important to appreciate that even if the spheres are touching and hence electrically connected, the dominant coupling between them is still capacitive because the resistance of a metal contact is extremely large at optical frequencies, since it is only at most a few ångströms in diameter and hence is substantially smaller than the mean free path of the electrons. Thus the *RC* time constant between two touching spheres is very large at optical frequencies. We estimate<sup>17</sup> that  $\omega \gg 1/RC$  by well over an order of magnitude, confirming the capacitive nature of the coupling.

The presence of all the remaining gold particles in the cluster can also have some effect upon the absorption. The sum of the fields of all the remaining particles acting on any given one will have the effect of changing the mean dielectric constant in an effective medium sense. However, the fractal structure of the aggregate means that the mean density of neighbouring particles decreases with distance. Thus we might expect the modification of the effective average dielectric constant to be quite small. To investigate this, we have performed a self-consistent calculation of the optical properties of the clusters using the computer simulations to obtain the exact coordinates of the particles.<sup>17</sup> The calculation is based on Ewald's self-consistent field method<sup>18</sup> in which the local exciting field at each particle site, including multipole scattering effects to all orders, is obtained exactly. The scattered field outside the cluster is then the sum of the radiation emitted by all the particles in the cluster while the absorption is obtained by summing the energy absorbed by each particle. Implicit in this approach is that the

polarizability of each gold particle is not given by the expression for a sphere in vacuum. Rather, it is calculated by taking into account all the near-field effects arising from higher-order multipole interactions between the nearest-neighbour spheres. These calculations confirm that the change in the effective average dielectric constant within the cluster is rather small, only *ca.* 5%, owing to the relatively low density of gold particles in the fractal structure.

Thus the absorption resonances of the aggregated gold colloids are dominated by the strong short-range correlations characteristic of the clusters, with the long-range fractal structure having relatively little influence. While the behaviour of the resonances of a dimer can serve as a qualitative guide, the actual behaviour of real aggregates is considerably more complicated. The short-range structure consists of a combination of chains of gold particles of varying lengths, oriented in all directions. The resonances for each sphere would be determined by their exact local environment, and would include effects of at least the nearest neighbours, and presumably the next few spheres as well. Indeed, the spatial extent of the resonance would depend on the excitation frequency, and would be larger as the long-wavelength resonance is approached. The actual absorption spectrum is thus the result of the combination of the resonances of all the spheres, with their different local environments and orientations combining to cause the observed width.

## Scattering

The gold aggregates scatter much more light than the unaggregated colloid. This is due primarily to the increased size of the clusters. The unaggregated gold particles are much smaller than the wavelength of light, and are therefore relatively ineffective scatterers relative to a cluster of size comparable to a wavelength. We can also see from fig. 1 that the resonances have some effect on the scattering, since there are two peaks in the total scattering as a function of wavelength. This results from the increased polarizability of the spheres caused by the optical resonances. However, rather than considering the integrated scattering from clusters, it is more informative to consider the angular, or  $k$  vector, dependence of the scattering, where  $k = 4\pi n \sin(\theta/2)/\lambda$ , with  $n$  the index of refraction of the water and  $\theta$  the angle between the direction of the incident light and the direction of the scattered light, and  $\lambda$  the wavelength.

For fractal objects, the long-range correlations can result in the now familiar  $k^{-d_f}$  dependence in the scattering intensity, when  $kR_g \gg 1$ , where  $R_g$  is the radius of gyration of the cluster.<sup>19</sup> When  $kR_g \leq 1$  the scattering becomes independent of  $k$ , as the internal fractal structure is no longer probed. To include both regimes, we can represent<sup>20</sup> the scattering intensity from a single cluster as

$$I_M = M^2 S_M(k)$$

where

$$S_M(k) = 1/(1 + 2k^2 R_g^2/3d_f)^{d_f/2}.$$

This form has the required behaviour that it varies as  $M^2$  for small clusters or small angles and as  $M/k^{d_f}$  for larger clusters at larger angles. The angular dependence of the scattered light intensity is thus very useful in that it can both determine the fractal dimension of the aggregates at large  $kR_g$ , and the characteristic size of the clusters, averaged over the cluster mass distribution, at small  $kR_g$ .

The  $k^{-d_f}$  dependence of the scattered light reflects the Fourier transform of the fractal correlations of the particles within the clusters. This implicitly assumes that the field at each particle is simply proportional to the incident field at that position. However, the field at each particle is in fact the local field, which is the sum of the incident field

and the radiated field from all the other particles at the given particle position. Nevertheless, the scattering properly reflects the Fourier transform of the particle correlations for the values of  $k$  probed in light-scattering experiments, as we now show.

At any given gold particle within the cluster, the total local exciting field,  $E_L$ , can be represented as the sum of the incident field,  $E_0$ , and the total magnitude of the radiated fields of all the other particles within the cluster,  $E_R$ , at the given particle. Of course,  $E_R$  must be calculated self-consistently to properly include the effects of all the particles. However,  $E_R$  will always be proportional to the incident field. Thus we can express the local field at each gold particle within the cluster as  $E_L = \chi E_0$ , where  $\chi$  must be determined self-consistently. Furthermore, we can divide the response into  $\chi = \chi_{\text{ave}} + \chi_{\text{fluc}}$  where  $\chi_{\text{ave}}$  is the average value, and is the same at each particle, while  $\chi_{\text{fluc}}$  expresses the fluctuations in  $\chi$  and varies from particle to particle. The scattering intensity will then be proportional to the Fourier transform of the spatial correlations of this field. These correlations can be divided into three terms. The first term reflects the correlations of  $\chi_{\text{ave}} E_0$  with itself. This term will reflect the fractal correlations as it is proportional to the incident field at each particle. The constant of proportionality reflects the change in the average dielectric constant of the cluster, and will affect the magnitude, but not the  $k$ -dependence of the scattering intensity. The second term reflects the correlations of  $\chi_{\text{ave}} E_0$  with  $\chi_{\text{fluc}} E_0$ , and because  $\chi_{\text{fluc}}$  has random spatial fluctuations, this term will average to zero. The final term reflects the correlations of  $\chi_{\text{fluc}} E_0$  with itself. Since  $\chi_{\text{fluc}}$  varies randomly in space, it will not exhibit the correlations of the fractal structure. Indeed, we expect no long-range correlations whatsoever. Instead there will only be short-range correlations whose spatial extent will be on the order of a single-sphere radius. Thus, at  $k$  vectors probed in light-scattering measurements, this term will be independent of  $k$ . Furthermore its magnitude will in general be small, and therefore this term will not contribute significantly. Thus the local field corrections do not contribute to the angular dependence of the light-scattering intensity.

These qualitative ideas have been confirmed in a more quantitative fashion using the self-consistent field calculations with the computer-generated clusters.<sup>17</sup> We calculate the scattered field exactly, properly accounting for the corrections to the local field. This can then be compared to a calculation of the scattering using only the incident field. To compare to experimentally measured results, we average over orientations and sum over many different clusters. When this is done, there is no observable difference between the exact calculations and the ones excluding the local field corrections. In both cases the fractal correlations are reflected in the  $k^{-d_f}$  dependence of the scattered intensity when  $kR_g \gg 1$ . This confirms the results of our qualitative arguments above.

There is one feature unique to light scattering that does allow the effects of the short-range correlations of the local field to be probed. This is the depolarized scattering, or the intensity of scattered light polarized normal to the incident field. Depolarized scattering arises because of the anisotropy induced in the polarizability of each sphere due to the presence of the nearest neighbours. Since the incident field is polarized, the depolarized components can only consist of contributions from the corrections to the local field due to the other particles in the cluster. The  $k$  dependence of the depolarized scattering reflects the Fourier transform of the spatial correlations of the local field corrections. Thus the only contribution will arise from the correlations of  $\chi_{\text{fluc}} E_0$  with itself, where we now are considering the depolarized component of this quantity. Again, since these terms vary randomly in space, there will be correlations only on length scales of the order of a single-sphere radius, and the depolarized scattering should be isotropic in  $k$  over the range probed in light-scattering experiments. This is indeed observed as is shown in fig. 2, where both the polarized and depolarized light scattering are shown as a function of  $k$  on a logarithmic plot. The data were obtained from clusters prepared by DLCA, and were obtained using the 633 nm HeNe laser line. The polarized scattering exhibits fractal correlations, with the slope giving  $d_f = 1.77$ . By contrast, the depolarized

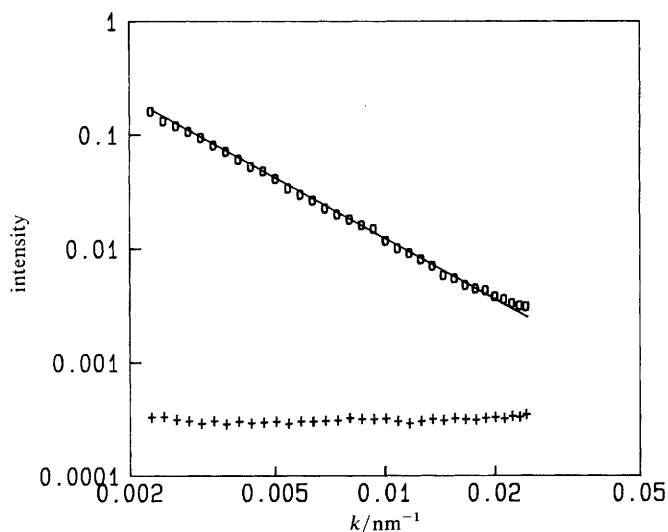


**Fig. 2.** Scattering intensity from diffusion-limited aggregated gold colloids as a function of  $k$ . The polarized scattering (upper curve) exhibits the linear behaviour on the logarithmic plot expected for the fractal correlations with  $d_f = 1.77$ . The depolarized scattering (lower curve) is isotropic.

scattering intensity is independent of  $k$ , reflecting the complete absence of correlations in the regime of  $k$  probed.

Since the depolarized scattering arises from the anisotropy of the polarizability of the spheres induced by the nearest neighbours, we would expect it to be strongly influenced by the electromagnetic plasma resonance. This is indeed observed, as can be seen by the variation in the intensity of the depolarized scattering with exciting wavelength. When the exciting wavelength is 488 nm, the depolarized intensity is very weak, on the order of 1% of the polarized intensity at high  $k$ . As the excitation wavelength is increased and approaches the second absorption resonance, the depolarized intensity also increases, and is *ca.* 6% of the high  $k$  polarized intensity at 633 nm and *ca.* 10% at 752 nm. This behaviour is consistent with the behaviour of the coupled electromagnetic plasma resonance. The long-wavelength resonance involves fields polarized parallel to the axis joining the spheres and will therefore induce the largest degree of anisotropy in the polarizability. Thus the magnitude of the depolarized scattering will increase as this resonance is approached.

Finally, we note that Schaefer and collaborators have claimed<sup>21</sup> that the fractal dimension of colloidal gold aggregates cannot be determined from light-scattering measurements because they are distorted by ‘multiple scattering effects’. The results of this section show that Schaefer’s argument is incorrect and confirm that it is based on an erroneous interpretation of his data.\*

### Dynamic Scattering

Dynamic, or quasielastic, light scattering<sup>22</sup> has proved quite useful in the study of the kinetics of the aggregation process. It measures the time dependence of the intensity fluctuations of the scattered light. Normally these fluctuations arise from the diffusional

\* Schaefer observed the slope of the scattering to change when he diluted his colloids. This was due to the shear-induced restructuring of the colloids upon dilution (see next section of this paper). Schaefer misinterpreted this to indicate ‘multiple scattering’ from the aggregates.

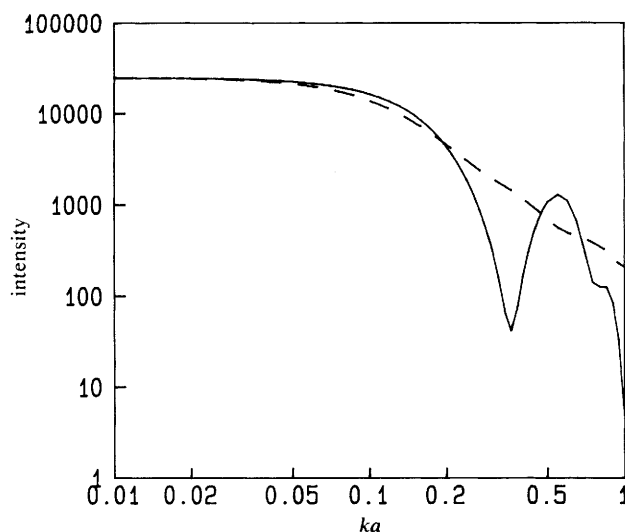


**Fig. 3.** The scattering intensity calculated for computer-generated DLCA clusters as a function of  $ka$  where  $a$  is the diameter of a single sphere. The solid line is the result for a single cluster of mass 500 particles in a single orientation, and exhibits large fluctuations when  $kR_g > 1$ . The dashed line is an average over 10 clusters and 100 randomly chosen orientations for each, and exhibits the expected linear, fractal behaviour when  $kR_g > 1$ .

motion of the particles in the scattering volume. However, for aggregated colloids, the size of the clusters can rapidly become much greater than  $k^{-1}$ , so that the scattering intensity from each cluster is no longer proportional to  $M^2$ , as it is for very small clusters. Nevertheless, since we know the structure of the clusters, we also know the mass dependence of the average scattering intensity. Indeed, if we use a scattering angle such that  $kR_g > 1$  for most of the clusters, the average scattered intensity from each cluster will scale as  $M$ . However, this dependence requires averaging over all orientations of the cluster. In actual fact, for a given orientation of a cluster, the scattering will not scale this way at all, and indeed will not even have the power-law dependence expected for a fractal. This is illustrated in fig. 3, where we have calculated the scattering from a computer-generated DLCA cluster comprised of 500 particles. We compute  $|\sum_i \exp(-\mathbf{k} \cdot \mathbf{r}_i)|^2$ , where the sum extends over all the particles in the cluster. The large oscillations in the scattering as a function of  $k$  are clearly visible, reflecting the highly disordered structure of the cluster. However, if we average the intensities from ten different clusters calculated for 100 randomly chosen orientations, we regain the expected power-law dependence, as shown by the dashed curve in fig. 3.

These results show the importance of the orientational averaging in determining the static scattering. However, we cannot ignore these variations in dynamic light scattering, as they will manifest themselves directly as fluctuations as the cluster undergoes rotational diffusion. This will add an additional decay mechanism in the autocorrelation of the scattered intensity. Physically, this arises from the fact that the cluster is larger than  $k^{-1}$  and so is comprised of many different blobs of size  $k^{-1}$ , whose scattering can interfere. The exact resultant intensity is then very sensitively dependent on the orientation of the cluster. One immediate consequence of this is that it is possible to see quasielastic scattering from a single cluster, even in a homodyne experiment.

To investigate the effects of rotational diffusion, we have developed a theory for the autocorrelation of the intensity fluctuations of inhomogeneous objects.<sup>23</sup> This theory is a generalization of the treatment for a long rod.<sup>22</sup> To apply our theory, we need to



know the position of all the particles in the clusters and thus use the computer-simulated cluster aggregates. We calculate the field-field correlation function for a set of rigid clusters made up of identical spheres. Experimentally we measure a homodyne intensity-intensity correlation function; in the limit of an infinite number of clusters, our measured correlation function will be the square of the field-field correlation function plus a baseline. If we have a small number of clusters in the scattering volume, this condition no longer holds. In this paper we deal only with the Gaussian limit of a large number of clusters, as it is usually achieved in our experiments.

For simplicity, the spheres are taken as point scatterers (*i.e.* the form factor is 1). Then the field-field correlation function is

$$S(k, t) = \sum_{\alpha, \beta} \sum_{i=1}^{n_{\alpha}} \sum_{j=1}^{n_{\beta}} \langle \alpha_0^2 \exp \{-i\mathbf{k} \cdot [\mathbf{r}_i^{\alpha}(t) - \mathbf{r}_j^{\beta}(0)]\} \rangle \quad (1)$$

where  $\mathbf{r}_i^{\alpha}(t)$  is the position of particle  $i$  in cluster  $\alpha$  at time  $t$ ,  $n_{\alpha}$  is the number of particles in cluster  $\alpha$ , and  $\alpha_0$  is the polarizability of each particle.

We now make some simplifying assumptions. We assume that our sample is sufficiently dilute so there are no correlations between clusters. We assume that the clusters are not too anisotropic, so we may represent translational diffusion of a cluster with a single diffusion coefficient,  $D_{\alpha} = k_B T / 6\pi\eta R_h$ , where  $\eta$  is the viscosity of water and  $R_h$  is the hydrodynamic radius of a cluster. Finally, we assume that translational and rotational diffusion are independent. This means that we may decompose the motion of the particles into the motion of the centre of mass of each cluster, which will depend on translational diffusion, and the motion of each particle about the centre of mass of its cluster, which depends on rotational diffusion. We then separate terms in the autocorrelation function and write it as

$$S(k, t) = \alpha_0^2 \sum_{\alpha} \exp(-D_{\alpha} k^2 t) \sum_{i,j} \langle \exp \{-i\mathbf{k} \cdot [\mathbf{b}_i^{\alpha}(t) - \mathbf{b}_j^{\alpha}(0)]\} \rangle \quad (2)$$

where  $\mathbf{b}_i^{\alpha}(t)$  is the displacement of particle  $i$  from the centre of mass of cluster  $\alpha$ . The first exponential reflects the decay in the autocorrelation function due to the centre-of-mass motion, while the second contains the rotational component. To calculate the rotational contribution, we expand the positions of the particles in each cluster as a series of multipole moments, and calculate the scattering from each moment. For each cluster we use a single rotational diffusion coefficient,  $\theta_{\alpha} = k_B t / 8\pi\eta R_h^3$ . The rotational contribution can then be expressed as a sum over these multipole moments;

$$\sum_{l=0}^{\infty} S_l^{\alpha}(k) \exp[-l(l+1)\theta_{\alpha} t] \quad (3)$$

where

$$S_l^{\alpha}(k) = \sum_{M=-l}^l \left| \sum_i j_l(kb_i^{\alpha}) Y_{lM}(\Omega_i^{\alpha}) \right|^2 \quad (4)$$

where  $j_l$  is the  $l$ th order spherical Bessel function,  $Y_{lM}$  are the spherical harmonics and  $\Omega_i^{\alpha}$  is the angle of displacement of particle  $i$  relative to an arbitrary axis of cluster  $\alpha$ . Combining the translational and rotational terms, the field-field correlation function is

$$S(k, t) = \alpha_0^2 \sum_{\alpha} \exp(-D_{\alpha} k^2 t) \sum_{l=0}^{\infty} S_l^{\alpha}(k) \exp[-l(l+1)\theta_{\alpha} t]. \quad (5)$$

The rate of decay due to translational diffusion depends on  $k^2$ , while rotational diffusion is independent of wavevector; however, the relative magnitude of each multipole term will vary considerably with  $k$ . Thus the effects of rotational diffusion will alter the  $k$  dependence of the decay of the autocorrelation function.

Using the computer-generated clusters, we calculate the  $S_l^{\alpha}(k)$  terms, and sum to obtain the correlation function. In fig. 4 we plot  $S_l(k)$  as a function of  $k$  averaged over

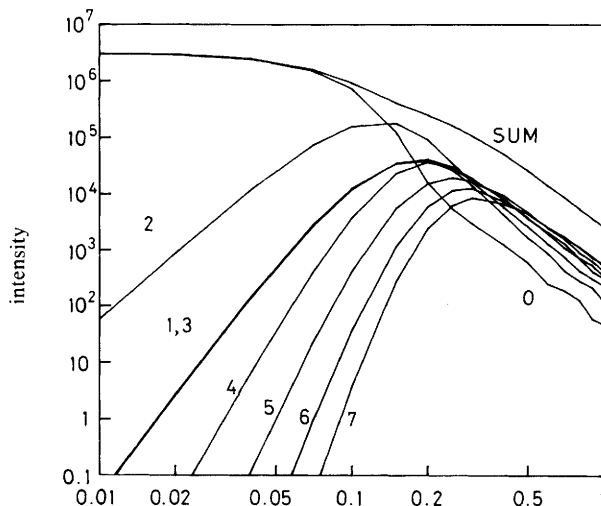


**Fig. 4.** Contributions of the spherical harmonics from  $l = 0$  to 7 to the scattering intensity calculated for 39 computer-generated clusters of mass 900 particles. The  $l = 0$  term only contributes to the translational decay of the autocorrelation function, while the  $l > 0$  terms also contribute to the rotational decay. The static scattering is the sum of all the terms.

39 900 particle clusters, for  $l = 0$  to 7. For  $kR_g \leq 1$  only the  $S_0$  term contributes, and the decay will be that expected for purely translational diffusion. Physically this reflects the fact that at small wavevectors the cluster scatters as a point, so the orientation of the cluster is irrelevant. As  $kR_g \geq 1$  we can distinguish regions within the cluster, so orientation is important. For these  $k$  values the higher-order  $S_l$  terms become important, and so rotational diffusion makes a greater contribution to the total decay of the autocorrelation function.

To compare our calculated results with experiment, we consider the  $k$  dependence of the first cumulant,  $\Gamma$ , which is the logarithmic derivative of the autocorrelation function as  $t \rightarrow 0$ . We use an ensemble of computer-generated clusters with a distribution similar to that produced experimentally by DLCA, and calculate  $\Gamma$  as a function of wavevector. To determine the rotational contributions, we use  $R_h = 0.8R_g$ ,<sup>†</sup> as determined numerically for the computer-generated clusters.<sup>24</sup> We compare the calculations with experimental results in fig. 5, where we have divided  $\Gamma$  by  $k^2$  to remove the simple dependence on  $k$ . For a purely translational system,  $\Gamma/k^2 = \bar{D}_0$ , the mean translational diffusion constant for the distribution of clusters. Our theoretical values for  $\Gamma/k^2$  approach  $\bar{D}_0$  at small wavevectors, and increase by a factor of *ca.* 2 at large  $k$ , showing the significant contribution due to rotational diffusion. We note that some of the  $k$  dependence of  $\Gamma$  is due to the fact that we are measuring different moments of the cluster mass distribution as  $S_M(k)$  changes as  $k$  is varied, but most of the  $k$  dependence is due to rotational effects. The data points in fig. 5 are experimentally measured first cumulants for DLCA aggregates with roughly the same size as our model clusters. The agreement of our calculation with the data is quite satisfactory. The calculations suggest that most of the variation in the experimentally measured decay with wavevector is due to rotational effects, although other effects may also contribute. Finally, we note that while a major contribution to  $\Gamma$  still comes from the  $\exp(-Dk^2t)$  term, due to translational diffusion, as  $kR_g$  increases rotational diffusion plays an increasingly important role in quasielastic light scattering.

<sup>†</sup> We thank Dr P. N. Pusey for pointing out an error in the ratio  $R_h/R_g$  used in the original version of this paper (see Discussion).

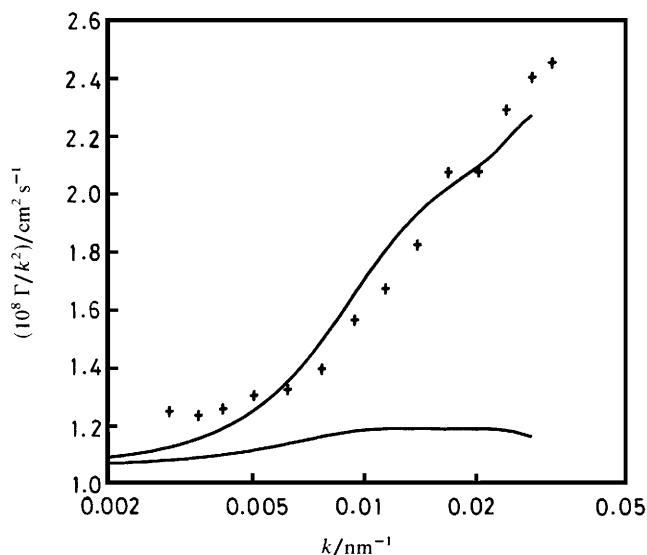


**Fig. 5.** The  $k$  dependence of the first cumulant, normalized by  $k^2$ , for a distribution of DLCA clusters. The solid line is the calculated behaviour, including effects of rotational diffusion. The points are experimental values.

### Mechanical Properties

All of the aggregates we have discussed so far have been formed under simple aggregation conditions, without the presence of additional forces of any sort. However, very often subsequent processing of flocs will subject the aggregates to a wide variety of stresses. We might expect the clusters to be quite susceptible to deformation, given their very tenuous nature. Indeed, a recent calculation of the mechanical properties of colloidal aggregates found that they could possess a fractal structure only up to some critical size when they become unstable to either thermal fluctuations or gravitational distortion.<sup>25</sup> In this section we discuss the effects of shear on the structure of the aggregates and the consequences on the static scattering from them.

To apply a controlled amount of shear to the clusters, they were first aggregated by DLCA until the characteristic cluster radius was *ca.* 5000 Å, as measured by dynamic light scattering. Then they were flowed through a narrow tube with various pressure drops across the length of the tube to change the flow velocity. The  $k$  dependence of the static scattering from the clusters was then compared with that obtained from the same colloid not subjected to shear. An example of the results obtained is shown in a logarithmic plot in fig. 6. The lower curve is from the unsheared aggregates, and exhibits the expected linear behaviour giving  $d_f = 1.84$ . By contrast, the scattering from aggregates subjected to a maximum shear of *ca.*  $10^4$  Hz, shown in the upper curve, no longer exhibits a simple linear shape. Instead, there is a distinct kink in the curve at  $k \approx 0.006 \text{ nm}^{-1}$ , which corresponds to a length of *ca.* 1700 Å. At larger  $k$  the scattering still has the same slope as that from the unsheared clusters. However, at small  $k$  the slope of the scattering has markedly increased, although it is not really possible to even describe it as linear on the logarithmic plot given the limited range of  $k$  probed.

The change in the scattering results from shear-induced restructuring of the tenuous fractal structure of the clusters. A plausible picture of the effects of the shear is that it causes the fractal aggregates to bend or deform, causing loops to be formed, thus strengthening the structure. These loops would tend to be formed on larger length scales, where the forces are greater and the structure weaker. Indeed, X-ray scattering

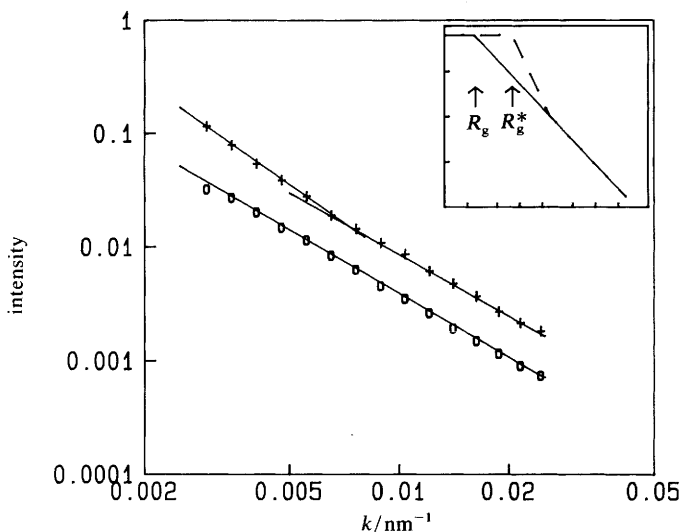


**Fig. 6.** Scattering from DLCA clusters before (lower curve) and after (upper curve) being subjected to shear. The shear causes restructuring of the fractal shape, changing the slope of the scattering at low  $k$ . The inset shows schematically the expected effect of the restructuring on the scattering.

from gold aggregates, which probes higher values of  $k$  than those observed with light, suggests that the fractal structure at small length scales is much more robust, and the restructuring occurs primarily at larger lengths.<sup>14</sup>

The expected effects of this restructuring on the scattering from the aggregates is shown schematically in the insert of fig. 6. The unsheared aggregates exhibit a linear behaviour in the fractal regime, with  $I \propto k^{-d_f}$ , until  $kR_g \approx 1$ , at which point the scattering becomes independent of  $k$ . Here,  $R_g$  represents an average radius of gyration of the clusters in the distribution. The intensity of the scattering at low  $k$  will be proportional to  $M^2$  averaged over the cluster distribution. Since this does not change upon shearing, the scattering from the sheared sample will have the same intensity at very low  $k$ . Furthermore, if the small length scale structure is robust and remains fractal, the scattering at high  $k$  will also be unchanged. However, the formation of loops will result in a decrease in  $R_g$ , so that the isotropic region of the scattering will have to extend to larger  $k$ . Then, to join properly with the scattering from the fractal region, the scattering in the region of  $k$  which probes length scales that have been substantially restructured will have to have a larger slope, as shown by the dashed line in the inset of fig. 6. If this region matches that probed in our light-scattering experiments, this simple argument would account for the behaviour observed.

An important consequence of this picture is that the restructured aggregates are not necessarily fractal at all on the length scales over which they are restructured. The scattering would neither be linear on a logarithmic plot nor would it approach any well defined slope. This is indeed what we observe: the apparent slope of the low  $k$  scattering varies with the magnitude of the applied shear. Furthermore, it does not always appear to be linear, although we rarely can probe over a sufficient range in  $k$  to determine this unambiguously. We note that these observations are in contrast with those for silica colloids.<sup>26</sup>

While our results are still preliminary, we can summarize the qualitative features as follows: as the shear increases, the restructuring extends to shorter length scales, as determined by the position of the change in slope in the scattering. Greater shear also

apparently leads to an increase in the apparent slope of the scattering in the region of  $k$  probing the restructured shape. Finally, the aggregates prepared by DLCA are considerably more susceptible to restructuring than those prepared by RLCA. The latter can exhibit some restructuring effects, but require substantially larger shear. This is consistent with the idea that the larger fractal dimension of the RLCA clusters,  $d_f \approx 2.1$ , results in a more robust structure.

### Conclusion

To summarize, we have found that the optical absorption of gold colloidal aggregates is dominated by the electronic plasma resonances in the gold spheres, which change from a single resonance in the unaggregated colloid to a pair of resonances in the aggregates due to the electromagnetic interactions between neighbouring spheres. The polarized scattering from the aggregates is dominated by the fractal structure of the clusters, giving a static structure factor  $S(k) \propto k^{-d_f}$ . The local field corrections due to the neighbouring particles have no effect on the  $k$  dependence of the polarized scattering. By contrast, the depolarized scattering is independent of wavevector, and reflects the short range of the spatial correlations of the corrections to the local field due to the other particles in the cluster. In dynamic light scattering we find that rotational diffusion can make a significant contribution to the decay of the autocorrelation function of the scattered light for  $kR_g \geq 1$ , but translational diffusion remains dominant for all wavevectors. Finally, we find that large clusters are subject to restructuring under mechanical stress. At large length scales, where the clusters are weakest, diffusion-limited clusters lose their original fractal behaviour. By contrast, reaction-limited clusters also restructure, but to a significantly lesser degree, owing to their higher initial fractal dimension.

### References

- 1 D. A. Weitz, M. Y. Lin, J. S. Huang, T. A. Witten, S. K. Sinha and J. S. Gethner, in *Scaling Phenomena in Disordered Systems*, ed. R. Pynn and A. Skjeltorp (Plenum, New York, 1985), p. 171.
- 2 D. A. Weitz and M. Oliveria, *Phys. Rev. Lett.*, 1984, **52**, 1433.
- 3 P. Meakin, *Phys. Rev. Lett.*, 1983, **51**, 1119.
- 4 M. Kolb, R. Botet and R. Jullien, *Phys. Rev. Lett.*, 1983, **51**, 1123.
- 5 D. A. Weitz, J. S. Huang, M. Y. Lin and J. Sung, *Phys. Rev. Lett.*, 1985, **54**, 1416.
- 6 D. A. Weitz, M. Y. Lin and C. J. Sandroff, *Surf. Sci.*, 1985, **158**, 147.
- 7 J. A. Creighton, C. G. Blatchford and M. G. Albrecht, *J. Chem. Soc., Faraday Trans. 2*, 1979, **75**, 790.
- 8 M. Kolb and R. Jullien, *J. Phys. Lett.*, 1984, **45**, L977.
- 9 W. D. Brown and R. C. Ball, *J. Phys. A*, 1985, **18**, L517.
- 10 R. C. Ball, D. A. Weitz, T. A. Witten and F. Leyvraz, *Phys. Rev. Lett.*, 1987, **58**, 274.
- 11 D. A. Weitz and M. Y. Lin, *Phys. Rev. Lett.*, 1986, **57**, 2037.
- 12 D. A. Weitz, J. S. Huang, M. Y. Lin and J. Sung, *Phys. Rev. Lett.*, 1984, **53**, 1657.
- 13 P. Meakin, *J. Colloid Interface Sci.*, 1984, **102**, 491.
- 14 P. Dimon, S. K. Sinha, D. A. Weitz, C. R. Safinya, G. S. Smith, W. A. Varaday and H. M. Lindsay, *Phys. Rev. Lett.*, 1986, **57**, 595.
- 15 P. K. Aravind, A. Nitzan and H. Metiu, *Surf. Sci.*, 1981, **110**, 189.
- 16 R. Landauer, in *Electrical Transport and Optical Properties of Inhomogeneous Media* (American Institute of Physics, New York, 1978), p. 2.
- 17 Z. Chen, P. Sheng, D. A. Weitz, H. M. Lindsay, M. Y. Lin and P. Meakin, to be published.
- 18 M. Lax, *Rev. Mod. Phys.*, 1951, **23**, 287.
- 19 D. W. Schaefer, J. E. Martin, P. Wiltzius and D. S. Cannell, *Phys. Rev. Lett.*, 1984, **52**, 2371.
- 20 G. Deitler, C. Aubert, D. S. Cannell and P. Wiltzius, *Phys. Rev. Lett.*, 1986, **57**, 3117.
- 21 J. P. Wilcoxon, J. E. Martin and D. W. Schaefer, in *Fractal Aspects of Materials* (Mat. Res. Soc. Extended Abstracts, 1985), p. 33, and unpublished.
- 22 B. J. Berne and R. Pecora, *Dynamic Light Scattering* (Wiley, New York, 1976).
- 23 H. M. Lindsay, R. Klein, M. Y. Lin, D. A. Weitz and P. Meakin, to be published.
- 24 P. Meakin, Z. Y. Chen and J. M. Deutch, unpublished.
- 25 Y. Kantor and T. A. Witten, *J. Phys. Lett.*, 1984, **45**, L675.
- 26 C. Aubert and D. S. Cannell, *Phys. Rev. Lett.*, 1986, **56**, 738.